Research Square

Preprints are preliminary reports that have not undergone peer review.
They should not be considered conclusive, used to inform clinical practice,
or referenced by the media as validated information.

Hybrid Reinforcement of Concrete with Recycled Tyre Steel Fibres and Lathe Metallic Shavings: Mechanical Performance and Carbon Footprint

Ahmad Subhan
Bahauddin Zakariya University
Mirza Shariq
mamjad.ms23nice@student.nust.edu.pk
National University of Sciences and Technology (NUST)
Naveed Ahmad
National University of Sciences and Technology (NUST)
Fatima Mehwish
Muhammad Nawaz Sharif University of Engineering & Technology

Research Article

Keywords: Recycled tyre steel fibres, Metallic shavings, Hybrid fibre reinforcement, Waste-derived reinforcement, Double-punch test, Splitting tensile strength, Flexural strength, Embodied carbon

Posted Date: November 25th, 2026

DOI: https://doi.org/10.21203/rs.3.rs-11649386/v1

License: This work is licensed under a Creative Commons Attribution 4.0 International License.
Read Full License

Additional Declarations: No competing interests reported.

Hybrid Reinforcement of Concrete with Recycled Tyre Steel Fibres and Lathe Metallic Shavings: Mechanical Performance and Carbon Footprint

Ahmad Subhan[a], Mirza Shariq [b!], Naveed Ahmad [b] , Fatima Mehwish[c]

[a] *Department of Civil Engineering, Bahauddin Zakariya University, Multan, Pakistan*

[b] *NUST Institute of Civil Engineering, School of Civil and Environmental Engineering (SCEE), National University of Science and Technology (NUST), H-12, Islamabad, Pakistan.*

[c] *Muhammad Nawaz Sharif University of Engineering and Technology Multan Pakistan*

---

*__Corresponding Author__
Mirza Shariq Amjad .
Research Associate
NUST Institute of Civil Engineering (NICE/SCEE),
National University of Sciences and Technology (NUST), H-12, Islamabad, Pakistan.
Email address: mamjad.ms23nice@student.nust.edu.pk
ORCID: 0009-0002-8988-7586

Abstract

Steel wastes from end-of-life tyres and machining are abundant, yet as concrete reinforcement they have mostly been studied separately and in dissimilar matrices. This study compared recycled tyre steel fibres (RTSF, cut bead wire, 25 mm), lathe-generated metallic shavings (MS) and equal-volume RTSF-MS hybrids in one normal-strength concrete (water-cement ratio 0.5). Ten mixtures comprised a control and three series at total fibre contents of 0.5, 1.0 and 1.5%. Slump and 28-day compressive, splitting tensile, double-punch tensile and four-point flexural strengths were measured, with a cradle-to-gate CO_2 assessment. At 1.5% fibre, slump fell from 90 mm to between 55 mm (hybrid) and 65 mm (RTSF). Compressive strength changed little with single fibres (at most +8.2%) but rose 15.1% with the hybrid. Splitting, double-punch and flexural strengths increased by 26.9, 21.9 and 24.4% with RTSF, by 19.2, 14.5 and 18.5% with MS, and by 44.6, 36.5 and 38.3% with the hybrid. In all twelve comparisons the hybrid exceeded the mean of its two single-fibre mixtures at equal dosage (hybrid effect index 1.04 to 1.18), which is compatible with complementary action of the two fibres, although significance was not tested (three specimens, one batch). Under a cut-off allocation, fibres left emissions at about 400 to 402 kg CO_2/m^3 but lowered carbon intensity by up to 13.5% per MPa of compressive and 28.0% per MPa of flexural strength. Relative to industrial steel fibres at equal dosage, the waste fibres avoided about 27 to 226 kg CO_2/m^3, depending on dosage and steelmaking route. The 1.0% hybrid matched or exceeded the 1.5% RTSF mixture with one third less fibre. Post-cracking behaviour and durability were not assessed.

Keywords: Recycled tyre steel fibres; Metallic shavings; Hybrid fibre reinforcement; Waste-derived reinforcement; Double-punch test; Splitting tensile strength; Flexural strength; Embodied carbon

1. Introduction

Concrete is the most widely used construction material, and the cementitious matrix that gives it high compressive capacity also makes it brittle in tension. Its tensile strength is typically of the order of one tenth of its compressive strength, and once a crack forms it propagates with little additional energy absorption [1, 2]. In most structures this weakness is handled with continuous bar reinforcement, which acts only after cracks have opened across the bars. Discrete fibres distributed through the matrix work at an earlier stage and at a smaller scale, intercepting cracks close to where they initiate.

Steel fibres are the most established form of discrete reinforcement. They bridge cracks, transfer stress across them and delay their coalescence, which raises the tensile and flexural capacity of the composite and, more markedly, its post-cracking resistance and toughness [3, 4]. The size of the benefit depends on fibre geometry, volume fraction and matrix strength. In high-strength concrete, for example, Song and Hwang [5] reported that the splitting tensile strength nearly doubled at 2% fibre by volume while compressive strength rose by roughly 15%, and similar dependence on aspect ratio and dosage has been reported elsewhere [6, 7]. Industrial steel fibres, however, are drawn and shaped from steel wire, adding cost and embodied emissions to a material whose cement content already dominates its carbon footprint [8]. Interest has therefore grown in steel that already exists in a fibre-like form within waste streams.

Recycled tyre steel fibres (RTSF) are the most studied of these. Passenger and truck tyres contain high-carbon steel in the form of multi-filament cords in the belt and carcass and thicker bead wires at the rim. Mechanical shredding, cryogenic processing or pyrolysis releases this steel as a mixture of short cords and single filaments of varying length, with a variable amount of rubber still attached [9-11]. Bead wire recovered separately is thicker and stiffer [12]. The resulting fibres therefore differ from industrial fibres in three respects that matter for concrete: their length and diameter are distributed rather than fixed, their shape is irregular and often bent, and they lack engineered end anchorage. Pull-out tests reported by Aiello et al. [13] indicated that the bond-slip response of recycled tyre fibres depends strongly on this irregular geometry.

The most consistent benefit of RTSF is in the post-cracking regime. Tlemat et al. [14] derived stress-strain relationships showing a sustained residual tensile capacity for concrete with recycled fibres, and Neocleous et al. [10] examined how existing design guidance could be adapted to them. Centonze et al. [15] and Hu et al. [11] reported residual flexural strengths that, depending on dosage and fibre grading, approached those of industrial-fibre concrete. At the element level, RTSF have been shown to improve the fatigue performance of pavement concrete [16] and to contribute to shear resistance at low fibre contents [17]. The evidence is less uniform for other properties. Increases in splitting tensile strength have been reported by several authors [18, 19], but changes in compressive strength have generally been small and of inconsistent sign [18]. The post-cracking performance of RTSF has often been lower than that of hooked-end industrial fibres [18], and workability decreases with dosage [20]. Liew and Akbar [21] attributed much of this scatter to differences in fibre cleaning, length grading and

dosage definition. Dosage effects can also be non-monotonic. Higher contents increase the number of fibres crossing a potential crack but also promote clustering of long, thin filaments, and Ali et al. [19] found the highest compressive strength at 0.75% RTSF by volume, whereas splitting and flexural strengths continued to rise up to 1.5%. Questions also remain about durability, including corrosion of thin filaments near the surface [19].

Other waste streams, notably crumb rubber and recycled aggregate, have been widely studied as sustainable substitutes for natural aggregate in concrete, but they often reduce its mechanical strength [22]. Metallic shavings (MS), also called swarf or machining chips, are produced in turning, milling and drilling and are normally collected as scrap, often contaminated with cutting fluid, for cleaning and remelting [23]. Their curled, ribbon-like or helical shapes and machined, grooved surfaces suggest a possible role as micro-reinforcement, although the same oil contamination can reduce bond with the cement paste. In concrete, shavings have been used both as a partial replacement of fine aggregate [24-26], where their high density and angular shape can raise unit weight and, in several reports, compressive strength, and as a fibre-like addition [27, 28], where the expected mechanism is crack bridging and interlock. Małek et al. [27] reported increases of 13.9 to 36.3% in compressive strength, 7.1 to 18.2% in flexural strength and 4.2 to 38.4% in splitting tensile strength for lathe chips added at 0.33 to 0.99% of the concrete volume. Djebri et al. [29] found that 0.5% by volume did not compromise the self-compacting properties of a mixture and increased its compressive strength. Aslan et al. [30] reported higher load capacity and ductility in reinforced concrete beams containing metal chips, and Los Santos-Ortega et al. [28] found that lathe-waste fibres gave mechanical performance comparable to commercial fibres with a lower global warming potential. Other studies have reported little change or reductions once dosage, particle size or contamination exceeded a certain level [24], and chips tend to entangle and ball at higher contents. Because shaving geometry depends on the machining operation and is rarely characterised in detail, the published results are difficult to compare, and tensile tests other than flexure are seldom reported.

Hybrid reinforcement combines fibres that differ in size, stiffness or bond so that each acts where it is most effective. The underlying argument is that cracking is a multi-scale process. Microcracks form and coalesce before a macrocrack localises, and small, numerous fibres can delay the first stage while longer fibres bridge the second [31, 32]. Banthia and Gupta [32] and Banthia and Sappakittipakorn [33] showed that combinations of fibres of different lengths or diameters can produce toughness greater than that of either fibre alone at the same total volume,

a response described as synergy. Other studies found that hybridisation mainly improved flexural and splitting strength at low fibre contents [34] or that the benefit depended strongly on the fibre pair and the matrix [35]. For waste fibres, hybrid studies have focused on partly replacing industrial steel fibres with RTSF. Bjegović et al. [36] observed a positive interaction between industrial and recycled steel fibres, and Martinelli et al. [37] and Caggiano et al. [38] reported that recycled fibres could substitute part of the industrial fibre content with limited loss of post-cracking strength, provided their geometry was adequate. Zhong and Zhang [39] combined RTSF with polypropylene fibres. In these studies the evidence for synergy was mostly qualitative. Establishing a true hybrid effect requires comparing the hybrid with its individual components at the same total fibre volume, ideally against a rule-of-mixtures expectation, which few waste-fibre studies have done.

Three limitations of the existing literature are relevant here. First, RTSF and MS have almost always been examined separately and in different matrices, ranging from normal-strength and self-compacting concrete to ultra-high-performance mixtures, so their relative effectiveness cannot be judged from the published data. Second, dosage has been defined inconsistently, as a percentage of concrete volume, as a mass fraction of cement or as a replacement of fine aggregate, which changes both the fibre content and the matrix at the same time. Third, the hybrid studies involving RTSF have combined them with industrial steel fibres [36-38] or polypropylene fibres [39], not with machining waste. To the authors' knowledge, no study has compared RTSF, MS and their combination at equal total fibre volume and evaluated the resulting concrete under compressive, splitting, double-punch and flexural loading in one programme. The double-punch test, although sensitive to fibre-controlled tensile cracking [40], has rarely been applied to waste-fibre concrete. Without such a controlled comparison, it is not possible to say whether shavings add anything to RTSF, whether a hybrid performs better than either material at the same fibre volume, or what workability penalty accompanies it.

The question addressed in this study is therefore how RTSF, MS and their hybrid combinations influence the fresh and mechanical behaviour of concrete under a common experimental framework. A direct comparison is useful because the two materials differ in scale and shape. The tyre fibres used here were straight or slightly bent wires about 25 mm long, whereas the shavings were thin, curled ribbons of variable length. Hybrid fibre theory suggests that reinforcements of different scale can act at different stages of cracking [31, 32], but whether this applies to two low-cost, irregular waste materials has not been established. Testing each

material alone and in combination at the same total volume fraction separates the influence of fibre type from that of fibre quantity.

In the experimental programme, a single concrete mixture (400 kg/m3 cement, water-cement ratio 0.5) was reinforced with RTSF, MS or a 1:1 (by volume) RTSF-MS hybrid at total fibre volume fractions of 0.5, 1.0 and 1.5%. Slump was measured on the fresh mixtures, and compressive, splitting tensile, double-punch tensile and flexural strengths were determined at 28 days. The individual and hybrid series were compared with the plain control and with each other at equal fibre content, the internal consistency of the three tensile-related tests was examined, and a hybrid effect index was used to judge whether the combined response exceeded that expected from its components. A cradle-to-gate CO_2 assessment was also carried out, both for the concrete as produced and in comparison with an equal dosage of industrial steel fibres.

The study provides a like-for-like dataset for two waste-derived steel reinforcements and their combination in one normal-strength matrix. It includes the double-punch test, a quantitative description of the hybrid response, and a carbon assessment in which the allocation of the waste steel and the comparison with industrial fibres are stated explicitly. The work does not evaluate post-cracking toughness, durability or structural members, and its conclusions are limited accordingly.

2. Materials and experimental methodology

2.1. Materials

2.1.1. Cement, aggregates, water and admixture

Ordinary Portland cement of grade 53 conforming to PS 232:2008 (R) [41] was used in all mixtures; its chemical composition is given in Table 1. The fine aggregate was natural sand from Lawrencepur as shown in Figure 1 (b) with a particle size range of 0 to 4.75 mm, a specific gravity of 2.66, a water absorption of 1.1% and a fineness modulus of 3.2. The coarse aggregate was gravel from Sargodha with a particle size range of 4.75 to 20 mm, a specific gravity of 2.60 and a water absorption of 1.0%. Both aggregates were batched in the saturated surface-dry (SSD) condition, so no correction to the mixing water was required. Potable tap water, which is acceptable for mixing without further testing under ASTM C1602 [42], was used for mixing and curing. A polycarboxylate ether (PCE) based superplasticizer (Sika ViscoCrete 3110) was added at 0.5% of the cement mass, that is 2 kg/m^3, in all mixtures including the control.

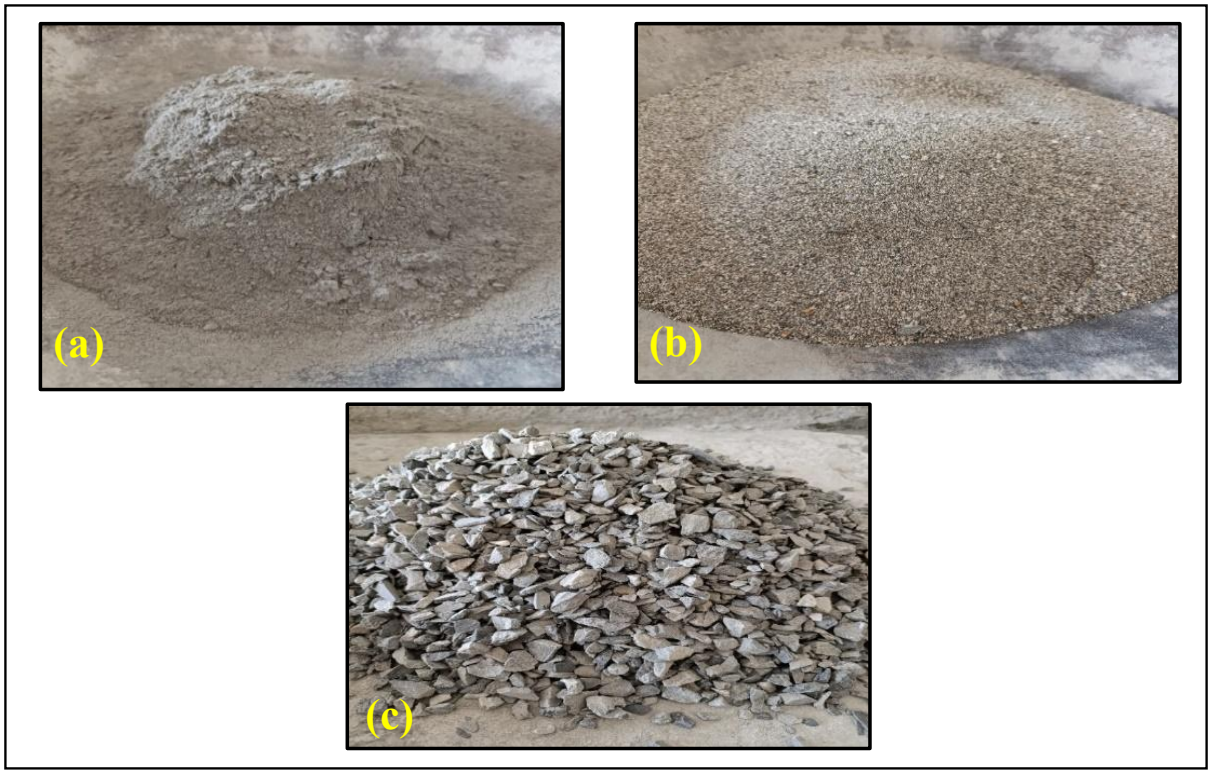


Figure 1 Materials, (a) Cement; (b) Sand; (c) Coarse Aggregate

Table 1. Chemical composition of the cement (% by mass).

Constituent	Content (%)
CaO	61.23
SiO_2	19.01
Al_2O_3	5.51
Fe_2O_3	3.41
MgO	3.31
SO_3	3.12
K_2O	0.97
Na_2O	0.19
Loss on ignition	3.25

2.1.2. Recycled tyre steel fibres

The RTSF were obtained from scrap dealers as steel wire recovered from discarded vehicle tyres. The recovered wires, initially up to about 1 m long, were cut to a nominal length of 25 mm (Figure 2). The measured wire diameter was 1.15 to 1.4 mm, which is in the range typical of tyre bead wire rather than the fine filaments of the belt cords [12]. The fibres were mostly straight, with some curved pieces, and had a generally smooth surface with local roughness.

No attached rubber was found on inspection; textile residue was not assessed. The density of the fibres, determined by the liquid-displacement method, was 7.81 g/cm^3.

The tensile strength of the RTSF was determined in accordance with ASTM E8/E8M [43]. Straight lengths of single wire were tested in their full cross-section, as the standard permits for wire of small diameter. A total of 100 wires were tested. Each specimen was held in serrated grips (grip length 4 mm) of a universal testing machine, with a gauge length of 20 mm, and loaded in uniaxial tension at a crosshead speed of 1 mm/min until fracture. The tensile strength was calculated as the maximum load divided by the original cross-sectional area, obtained from the diameter measured on each specimen. The mean tensile strength was 2200 MPa. The geometric and physical properties of the fibres are summarized in Table 2.



Figure 2. Recycled tyre steel fibres (RTSF) after cutting to a nominal length of 25 mm.

2.1.3. Metallic shavings

The metallic shavings were collected from lathe turning of ASTM A53 steel pipe [44] in local machine shops. They were curled, wavy or helical ribbons with machining grooves on the surface. Measurements on a sample of 100 to 200 pieces gave lengths of 9 to 40 mm, widths of 1.5 to 4.6 mm and thicknesses of 0.24 to 0.60 mm. Their density, determined by liquid displacement, was 7.84 g/cm^3. The tensile strength of the shavings was not measured directly. It was taken as that of the parent material, for which ASTM A53 specifies a minimum tensile strength of 330 MPa [44]. Because chip formation involves severe plastic deformation of the parent steel, the actual strength of the shavings may be higher, and this value should be read as a lower-bound indication.

Before use, the shavings were exposed to direct sunlight for 48 h to reduce residual cutting oil and coolant. The effectiveness of this treatment was judged visually, and the residual oil content was not quantified. No rubber or textile contamination was present.

Because the shavings are ribbons rather than round wires, their aspect ratio was calculated as the ratio of length to the equivalent diameter of a circle with the same cross-sectional area, $d_{eq} = (4wt/\pi)^{0.5}$, where w and t are the ribbon width and thickness. This gives aspect ratios of roughly 5 to 60 over the measured dimensional range. The corresponding values for RTSF, calculated from the nominal length and the measured diameter range, are about 18 to 22. The shavings therefore cover a much wider range of slenderness than the tyre fibres, which are short and comparatively stiff.

Table 2. Geometric and physical characteristics of the RTSF and metallic shavings (MS).

Parameter	**RTSF**	**MS**	**Basis**
Source	Discarded vehicle tyres (scrap dealers)	Lathe turning of ASTM A53 steel pipe	Supplier/collection record
Length (mm)	25 (nominal cut length)	9 to 40	Measured, 100 to 200 pieces
Width (mm)	Not applicable (round wire)	1.5 to 4.6	Measured
Diameter or thickness (mm)	1.15 to 1.4	0.24 to 0.60 (typical 0.4)	Measured
Aspect ratio (-)	approx. 18 to 22	approx. 5 to 60 (based on d_{eq})	Calculated from measured dimensions
Density (g/cm^3)	7.81	7.84	Measured, liquid displacement
Tensile strength (MPa)	2200	330 (parent steel)	RTSF: measured, ASTM E8/E8M; MS: ASTM A53 specification
Shape	Mostly straight, some bent	Curled, wavy or helical ribbons	Visual inspection
Surface	Smooth with local roughness	Machining grooves, rough face	Visual inspection
Rubber contamination	None observed	None	Visual inspection
Textile contamination	Not assessed	None	Visual inspection
Oil or coolant	Not applicable	Removed by 48 h sun exposure; residue not quantified	Treatment record; visual



(a) **(b)**

Figure 3. Metallic Shavings (a) Parent materials; (b) Extracted Shavings

2.2. Mix proportions and nomenclature

A single reference mixture with 400 kg/m^3 cement, 200 kg/m^3 water (water-cement ratio 0.5), 728 kg/m^3 fine aggregate, 1038 kg/m^3 coarse aggregate and 2 kg/m^3 superplasticizer was used as the control (CM) as shown in Table 3. Fibre contents were defined as volume fractions of the concrete, V_f, and converted to mass per cubic meter using the measured fibre density (1):

$$m_f = \rho_f V_f \quad (1)$$

where m_f is the fibre mass (kg/m^3), ρ_f is the fibre density (7810 kg/m^3 for RTSF and 7840 kg/m^3 for MS) and V_f is the fibre volume fraction. Nine fibre-reinforced mixtures were produced in three series (Table 3). In the RTSF and MS series, a single fibre type was used at V_f = 0.5, 1.0 and 1.5%. In the hybrid series, RTSF and MS were combined in equal volumes to give the same three total fibre contents, that is, 0.25 + 0.25%, 0.50 + 0.50% and 0.75 + 0.75%. The number in each mixture designation is the total fibre volume fraction in percent.

Cement, water and superplasticizer contents were held constant across all mixtures, so the water-cement ratio remained 0.5 throughout and differences between mixtures at the same total fibre content arise from fibre type alone. To accommodate the fibres, the fine and coarse aggregate contents were each reduced by approximately 1.1% of their reference values for every 0.5% increment in fibre volume fraction, applied identically in the three series. The volumetric consequence of this adjustment was checked by an absolute-volume calculation using the measured specific gravities of the aggregates and fibres and a specific gravity of 3.15 for cement. For the control, the cement, water, aggregates and superplasticizer occupy 981.8 L

per cubic metre, leaving 1.8% for entrapped air, which is consistent with the value of about 2% expected for non-air-entrained concrete with 20 mm aggregate [45]. Each 0.5% fibre increment removed about 7.6 L of aggregate while adding 5.0 L of fibre, so the absolute volume of the constituents decreased to 974.3 L at 1.5% fibre. The difference of 7.5 L (0.75% of the volume) implies either a marginally lower yield or a marginally higher air content. Either way, the effect is small: the effective fibre fraction at 1.5% would be 1.51% rather than 1.50%, and the cement content per unit of yielded concrete would change by less than 0.8%. These deviations are an order of magnitude smaller than the property changes measured between mixtures and do not affect the comparisons drawn in this study.

Table 3. Mix proportions (kg/m^3). Water-cement ratio 0.5 for all mixtures.

Mix ID	$V_{f,RTSF}$ (%)	$V_{f,MS}$ (%)	Cement	Water	Fine agg.	Coarse agg.	SP	RTSF	MS	Total
CM	0	0	400	200	728	1038	2	0	0	2368.0
RTSF-0.5	0.50	0	400	200	720	1026	2	39.05	0	2387.1
RTSF-1.0	1.00	0	400	200	712	1015	2	78.10	0	2407.1
RTSF-1.5	1.50	0	400	200	704	1003	2	117.15	0	2426.2
MS-0.5	0	0.50	400	200	720	1026	2	0	39.20	2387.2
MS-1.0	0	1.00	400	200	712	1015	2	0	78.40	2407.4
MS-1.5	0	1.50	400	200	704	1003	2	0	117.60	2426.6
RTSF-MS-0.5	0.25	0.25	400	200	720	1026	2	19.53	19.60	2387.1
RTSF-MS-1.0	0.50	0.50	400	200	712	1015	2	39.05	39.20	2407.3
RTSF-MS-1.5	0.75	0.75	400	200	704	1003	2	58.58	58.80	2426.4

SP = PCE superplasticizer (0.5% of cement mass). V_f = fibre volume fraction of the concrete. The number in each mix ID is the total fibre volume fraction (%); in the hybrid (RTSF-MS) mixtures, each fibre type provides half of it. Fibre masses were obtained from Eq. (1) with densities of 7.81 g/cm^3 (RTSF) and 7.84 g/cm^3 (MS).

2.3. Mixing, casting and curing

Each mixture was produced as a single batch in a mechanical concrete mixer. Coarse aggregate, fine aggregate and cement were first dry-mixed for 3 min. The mixing water, containing 50% of the superplasticizer, was then added slowly while mixing continued for 2 min, after which the remaining superplasticizer was added and mixed for a further 1 min. The fibres were introduced last into the wet mixture to limit balling: RTSF were added gradually over 2 to 3 min and MS over 1 to 2 min while the mixer was running. In the hybrid mixtures, the RTSF were added first, followed by the shavings.

Each batch was used to cast six cylinders of 101.6 mm diameter and 203.2 mm height (4 in × 8 in), three for compressive and three for splitting tensile testing; three cylinders of 152.4 mm diameter and 304.8 mm height (6 in × 12 in), each sawn in half to provide 152.4 mm × 152.4

mm (6 in × 6 in) specimens for the double-punch test, of which three were tested per mixture; and three beams of 101.6 mm × 101.6 mm × 508 mm (4 in × 4 in × 20 in) for flexural testing. Steel moulds were cleaned and oiled before casting. The moulds were filled in three layers and compacted on a vibrating table for 2 min; no rodding was used. The top surface was levelled with a trowel. The specimens were demolded after 24 h and cured by full immersion in water at room temperature (23 to 24 °C) until testing at 28 days. Figure 4 illustrates the schematic representation of casting and curing methodology.

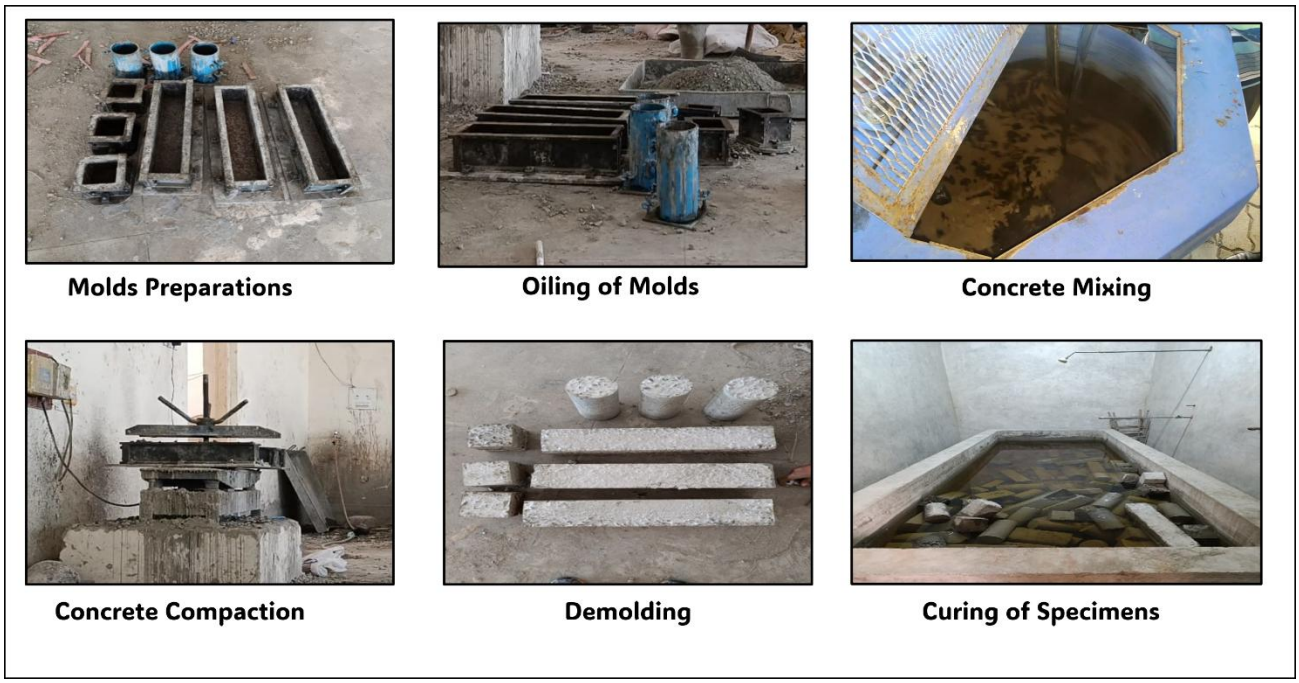


Figure 4. Specimens Preparations and Casting methodology

2.4. Test methods

The test programme is summarised in Table 4, and the loading arrangements are shown in Figure 5. All hardened-concrete tests were carried out in the concrete laboratory of the University College of Engineering and Technology, Bahauddin Zakariya University, using a universal testing machine for the cylinder tests and a flexural testing machine for the beams.

Table 4. Summary of the test programme.

Property	Method	Specimen	Age	Specimens per mixture
Slump	ASTM C143/C143M	Fresh concrete	Fresh	1 test
Compressive strength	ASTM C39/C39M, 0.25 MPa/s, no capping	Cylinder, 101.6 × 203.2 mm	28 d	3

Property	Method	Specimen	Age	Specimens per mixture
Splitting tensile strength	ASTM C496/C496M, 0.7 MPa/min	Cylinder, 101.6 × 203.2 mm	28 d	3
Double-punch tensile strength	Chen, punches 38.1 mm dia. × 25.4 mm, 1 kN/s	Cylinder, 152.4 × 152.4 mm (152.4 × 304.8 mm sawn in half)	28 d	3
Flexural strength	ASTM C78/C78M, four-point loading, span 450 mm, 1.0 MPa/min	Beam, 101.6 × 101.6 × 508 mm	28 d	3



Figure 5. Test arrangements: (a) compression; (b) splitting tensile test with bearing strips.

The consistency of each fresh mixture was measured with the standard slump cone in accordance with ASTM C143 [46] immediately after mixing.

2.4.2. Compressive strength

Compressive strength was determined on 101.6 mm × 203.2 mm cylinders at 28 days according to ASTM C39/C39M [47]. The specimens were tested after loose particles had been removed from the end faces. The load was applied continuously at a stress rate of 0.25 MPa/s, the central value of the range specified by ASTM C39/C39M. The compressive strength was calculated as (2);

$$f_c = P/A \quad (2)$$

where P is the maximum load (N) and A is the cross-sectional area of the cylinder (mm^2).

2.4.3. Splitting tensile strength

The splitting tensile strength was measured on 101.6 mm × 203.2 mm cylinders at 28 days according to ASTM C496/C496M [48]. Each cylinder was placed horizontally between the platens with plywood bearing strips along the top and bottom lines of contact, and the load was increased at a splitting stress rate of 0.7 MPa/min, within the range of the standard, until the specimen split along the loaded diameter. The splitting tensile strength was calculated as shown in Eq (3):

$$f_{ct} = 2P/(\pi LD) \quad (3)$$

where P is the maximum load (N), L is the specimen length (mm) and D is the specimen diameter (mm).

2.4.4. Double-punch tensile strength

The double-punch test proposed by Chen [49] was used as a second indirect tensile test. No ASTM or EN standard covers the plain-concrete version of this test; a related procedure for fibre-reinforced concrete, the Barcelona test, is standardised in Spain as UNE 83515 [40, 50]. The specimens were 152.4 mm × 152.4 mm cylinders obtained by sawing three 152.4 mm × 304.8 mm cylinders per mixture in half, so that each specimen had one molded and one sawn end face. Each specimen was placed vertically in the testing machine and loaded through two cylindrical steel punches, 38.1 mm in diameter and 25.4 mm thick, centered on its top and bottom faces (Figure 6 (a)). The punches bore directly on the concrete without packing. Under this arrangement the concrete beneath each punch forms a cone that wedges the specimen apart, and failure occurs by tensile splitting along several radial planes through the specimen axis. The load was increased uniformly at a rate of 1 kN/s until failure, and the double-punch tensile strength was calculated with Chen's limit-analysis expression shown in Eq (4) [49, 51]:

$$f_{dp} = P/[\pi(1.2bH - a^2)] \quad (4)$$

where P is the maximum load (N), a is the punch radius (19.05 mm), b is the specimen radius (76.2 mm) and H is the specimen height (152.4 mm). With these dimensions the punch-to-specimen diameter ratio is 0.25 and the height-to-diameter ratio is 1.0, which are the proportions of the 6 in × 6 in specimens and 1.5 in punches used by Chen [49] and for which Eq. (4) was derived. For this geometry the denominator of Eq. (4) equals 42,639 mm^2, so a

double-punch strength of 1 MPa corresponds to a peak load of about 42.6 kN Because the expression comes from a limit analysis and elastic analyses show that the stress field depends on the specimen proportions [52, 53], the double-punch strength is treated as an index of tensile capacity that is comparable between mixtures, and with other studies using the same geometry, but is not identical to the uniaxial tensile strength.



Figure 6 Test arrangement: (a) Double punch tensile test; (b)Cut Specimens after failure.

2.4.5. Flexural strength

The flexural strength (modulus of rupture) was determined on 101.6 mm × 101.6 mm × 508 mm beams at 28 days using four-point (third-point) loading according to ASTM C78/C78M [54] with the span modified. Each beam was simply supported over a span of 450 mm (about 4.4 times the beam depth, longer than the span of three times the depth specified by the standard) and loaded at the third points, 150 mm apart, so that the middle third of the span was subjected to a constant bending moment. The load was applied at a stress rate of 1.0 MPa/min, within the range specified by the standard, until rupture. For fracture within the middle third, the flexural strength was calculated as in Eq (5);

$$f_r = PL/(bd^2) \quad (5)$$

where P is the maximum load (N), L is the span (mm), and b and d are the width and depth of the beam (mm).

2.5. Carbon footprint assessment

2.5.1. Goal, scope and allocation

The CO_2 assessment was designed to answer two separate questions: whether adding waste steel changes the emissions of the concrete itself, and how the waste fibres compare with the industrial steel fibres they would replace in practice. It follows the framework of ISO 14040 and ISO 14044 [55, 56] and the modular structure of EN 15804 [57]. The declared unit is 1 m^3 of concrete, and the system boundary covers the production of the constituent materials (module A1, cradle to gate). Transport (A2) and batching and mixing (A3) were excluded because the same plant, mixer and placement were used for all mixtures.

Both RTSF and MS are wastes recovered after the end of their first life. Following the polluter-pays (cut-off) principle of EN 15804, a secondary material enters the product system free of the burdens of its previous life once it reaches the end-of-waste state; only the processing needed to prepare it for reuse is attributed to the new product [57]. Here that processing consisted of manual cutting of the tyre wire and solar drying of the shavings, neither of which uses purchased energy, so it was assigned zero emissions. A credit for the avoided emissions of scrap remelting was considered but not applied. Scrap that is diverted to concrete is not avoided production, because the steel it would have become must then be supplied by other routes, and EN 15804 does not allow a credit for secondary material entering a system. Retaining it would therefore have overstated the benefit.

3.5.2. Scenarios and emission factors

Two scenarios were evaluated. Scenario S1 (cut-off) quantifies the emissions of the concrete actually produced in Eq $E_{S1} = \Sigma\, m_i\, EF_i$ (6) :

$$E_{S1} = \Sigma\, m_i\, EF_i \tag{6}$$

where m_i is the mass of constituent i per cubic meter and EF_i is its emission factor (Table 5). The fibres carry no burden in S1. Scenario S2 (comparative substitution) asks what the same concrete would emit if the identical fibre dosage were supplied by industrial steel fibres (Eq $E_{S2} = E_{S1} + (m_{RTSF} + m_{MS}) \times EF_{steel}$ (7) :

$$E_{S2} = E_{S1} + (m_{RTSF} + m_{MS}) \times EF_{steel} \tag{7}$$

The difference E_{S2} - E_{S1} is the emission avoided by using waste rather than industrial fibres at the same dosage. Because the emission factor of industrial fibres depends on the steelmaking route, two bounding values were used: 0.69 kg CO_2/kg for scrap-based electric arc furnace (EAF) steel and 1.92 kg CO_2/kg for the global average of crude steel production in 2024 [58].

Both refer to crude steel and exclude wire drawing and fibre forming, so S2 underestimates rather than overstates the burden of industrial fibres. S2 also assumes equal dosage rather than equal performance; industrial fibres with end anchorage are usually more effective than recycled fibres [18, 59], so the equal-performance dosage of industrial fibres could be lower, and the avoided emissions would decrease accordingly.

The emission factors for cement, water, fine aggregate and superplasticizer were taken from Wu et al. [60] and that for coarse aggregate from Flower and Sanjayan [61]. To relate emissions to performance, the carbon intensity per unit strength (kg CO_2 m^{-3} MPa^{-1}) was calculated for S1 using the measured compressive and flexural strengths [62].

Table 5. Emission factors used in the carbon assessment.

Material	Emission factor (kg CO_2/kg)	Source
Cement	0.85	Wu et al. [60]
Water	0.000329	Wu et al. [60]
Fine aggregate	0.01172	Wu et al. [60]
Coarse aggregate	0.0459	Flower and Sanjayan [61]
Superplasticizer	3.09	Wu et al. [60]
RTSF, MS (S1, cut-off)	0	EN 15804 cut-off; processing without purchased energy
Industrial steel fibre, scrap-EAF route (S2)	0.69	worldsteel, 2024 data [63] [58].
Industrial steel fibre, global average (S2)	1.92	worldsteel, 2024 data [58].

S2 factors refer to crude steel and exclude wire drawing and fibre forming.

2.6. Data treatment

Each strength value reported in this study is the mean of three specimens. Changes relative to the control were calculated as $\Delta = (X_i - X_{CM})/X_{CM} \times 100\%$. To assess the hybrid response, a hybrid effect index (HEI) was defined as the ratio of the hybrid result to the mean of the two single-fibre results at the same total fibre volume fraction (Eq HEI = $X_{RTSF\text{-}MS}$ / [0.5(X_{RTSF} + X_{MS})] (8):

$$HEI = X_{RTSF\text{-}MS} / [0.5(X_{RTSF} + X_{MS})] \quad (8)$$

Because each hybrid contains equal volumes of the two fibres, the denominator is the linear rule-of-mixtures expectation for that hybrid. An HEI above 1.0 indicates that the combination performed better than a proportional blend of its components would predict; an HEI below 1.0 indicates the opposite [32].

3. Results and discussion

The measured properties of all mixtures are listed in Table 8, and their changes relative to the control are mapped in Figure 7. Two features stand out before the individual properties are discussed. The tensile-related properties responded much more strongly to fibre addition than compressive strength, and at every dosage the hybrid mixture gave the highest value of each strength property and the lowest slump.

Table 6. Fresh and 28-day mechanical properties (mean values). Values in parentheses are changes relative to CM (%).

Mix ID	Slump (mm)	f_c (MPa)	f_{ct} (MPa)	f_{dp} (MPa)	f_r (MPa)
CM	90	31.00	2.60	3.10	4.10
RTSF-0.5	84 (-6.7)	32.00 (+3.2)	2.80 (+7.7)	3.30 (+6.5)	4.30 (+4.9)
RTSF-1.0	76 (-15.6)	33.00 (+6.5)	3.20 (+23.1)	3.65 (+17.7)	4.70 (+14.6)
RTSF-1.5	65 (-27.8)	33.54 (+8.2)	3.30 (+26.9)	3.78 (+21.9)	5.10 (+24.4)
MS-0.5	85 (-5.6)	31.50 (+1.6)	2.80 (+7.7)	3.31 (+6.8)	4.23 (+3.2)
MS-1.0	71 (-21.1)	32.14 (+3.7)	3.00 (+15.4)	3.52 (+13.5)	4.59 (+12.0)
MS-1.5	63 (-30.0)	31.45 (+1.5)	3.10 (+19.2)	3.55 (+14.5)	4.86 (+18.5)
RTSF-MS-0.5	81 (-10.0)	33.00 (+6.5)	3.00 (+15.4)	3.49 (+12.6)	4.50 (+9.8)
RTSF-MS-1.0	66 (-26.7)	34.89 (+12.5)	3.50 (+34.6)	3.84 (+23.9)	5.23 (+27.6)
RTSF-MS-1.5	55 (-38.9)	35.67 (+15.1)	3.76 (+44.6)	4.23 (+36.5)	5.67 (+38.3)

f_c = compressive strength; f_{ct} = splitting tensile strength; f_{dp} = double-punch tensile strength; f_r = flexural strength (four-point loading).

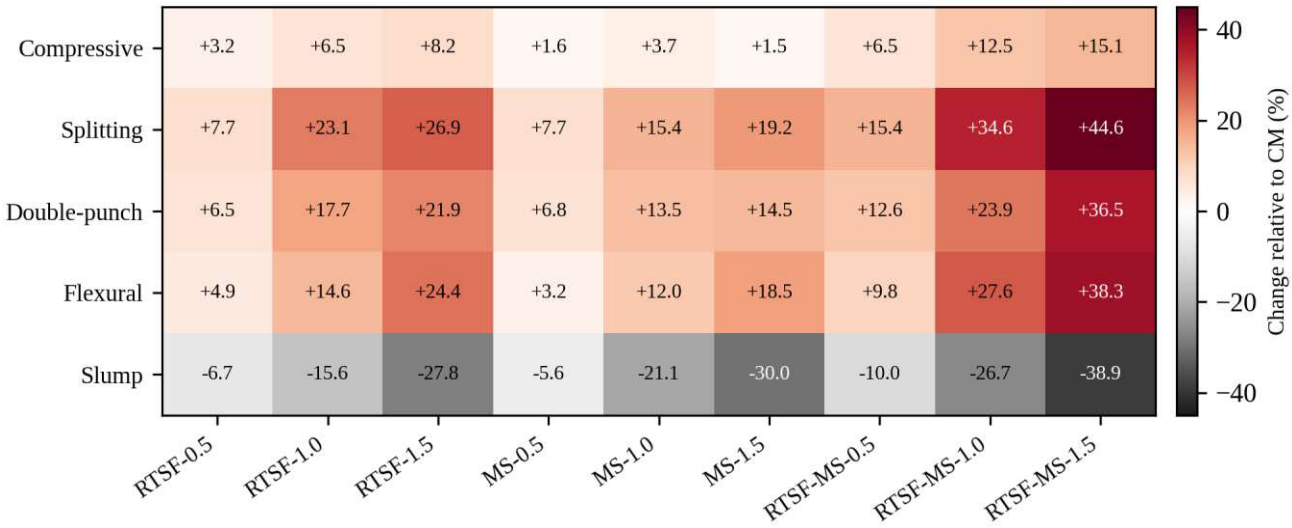


Figure 7. Change of each property relative to the control mixture (CM). Positive values indicate an increase

3.1. Workability

All fibres reduced the slump, and the reduction grew with fibre content (Figure 8). From 90 mm for the control, slump fell to 84, 76 and 65 mm in the RTSF series and to 85, 71 and 63 mm in the MS series at 0.5, 1.0 and 1.5% fibre. The hybrid series showed the largest losses, 81, 66 and 55 mm, corresponding to reductions of 10.0, 26.7 and 38.9%. Across the nine fibre mixtures, slump was strongly and negatively correlated with total fibre volume (r = -0.94), so fibre quantity was the dominant variable. At 0.5% the two single fibres behaved almost identically, whereas at 1.0 and 1.5% the shavings caused a slightly larger loss than the tyre fibres.

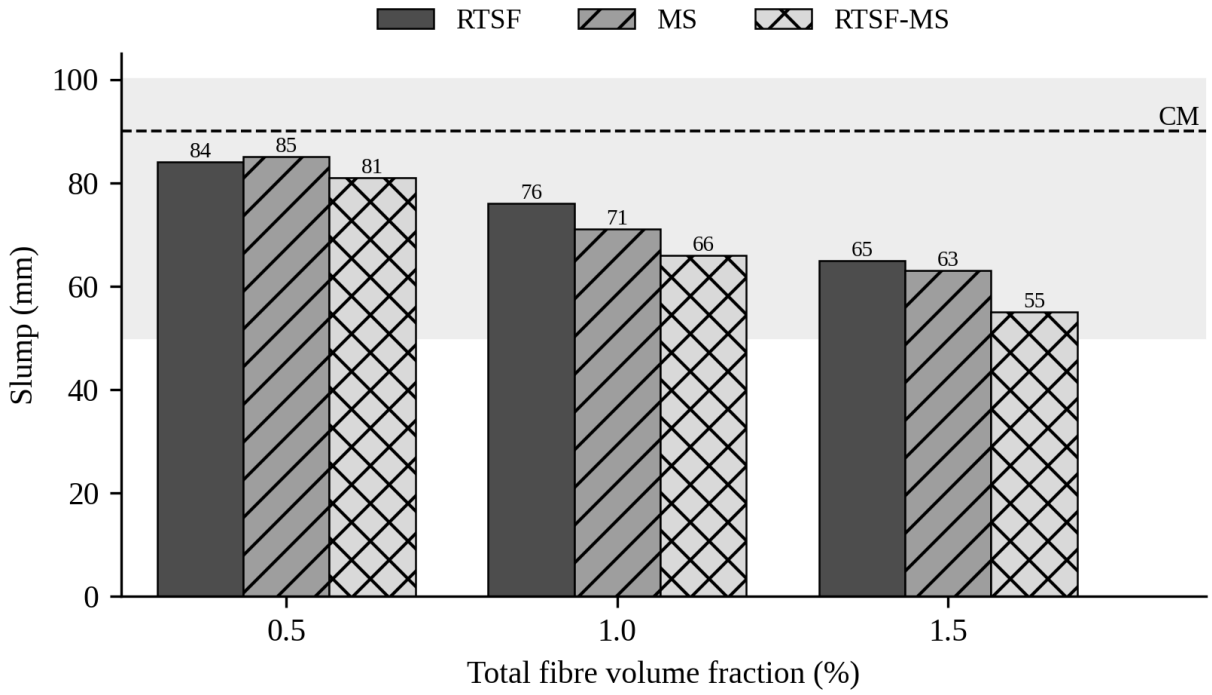


Figure 8. Slump of the fibre-reinforced mixtures. The dashed line is the control mixture; the shaded band marks the 50 to 100 mm range.

Steel fibres do not absorb water, so the loss of slump must be explained by their effect on the granular skeleton and on internal friction. Rigid fibres disturb the packing of the coarse aggregate and increase the amount of paste needed to fill the voids around them, and above a certain relative fibre content they form a connected network that resists flow [64, 65]. For the shavings, the curled and helical geometry and the serrated machined surface are likely to add mechanical interlock between neighboring pieces and with the aggregate, which would explain why their effect grew faster with dosage than that of the straighter RTSF. The hybrid mixtures lost more slump than the mean of the corresponding single-fibre mixtures, by factors of 0.96, 0.90 and 0.86 at 0.5, 1.0 and 1.5%. One plausible explanation is that the curls of the shavings entangle with the straight tyre wires, forming a more connected fibre network than either

material forms alone. This mechanism was not observed directly and should be regarded as a hypothesis.

In practical terms, all mixtures remained in the 50 to 100 mm range and were compacted by vibration without difficulty in the laboratory. Slump is, however, a measure of yield stress under self-weight and does not fully describe the compactability of fibre-reinforced concrete under vibration [3]. The 55 mm slump of the 1.5% hybrid should therefore be seen as a warning that, at higher dosages or in congested elements, the superplasticizer content or the paste volume would need adjusting.

3.2. Compressive strength

Compressive strength was modestly affected by fibre addition (Figure 9 (a)). In the RTSF series it increased progressively with dosage from 31.0 MPa to 32.0, 33.0 and 33.54 MPa, a maximum gain of 8.2%. The MS series showed only small changes, 31.5, 32.14 and 31.45 MPa, with the highest value at 1.0% and a return to near-control strength at 1.5%. The hybrids gave 33.0, 34.89 and 35.67 MPa, or 6.5, 12.5 and 15.1% above the control.

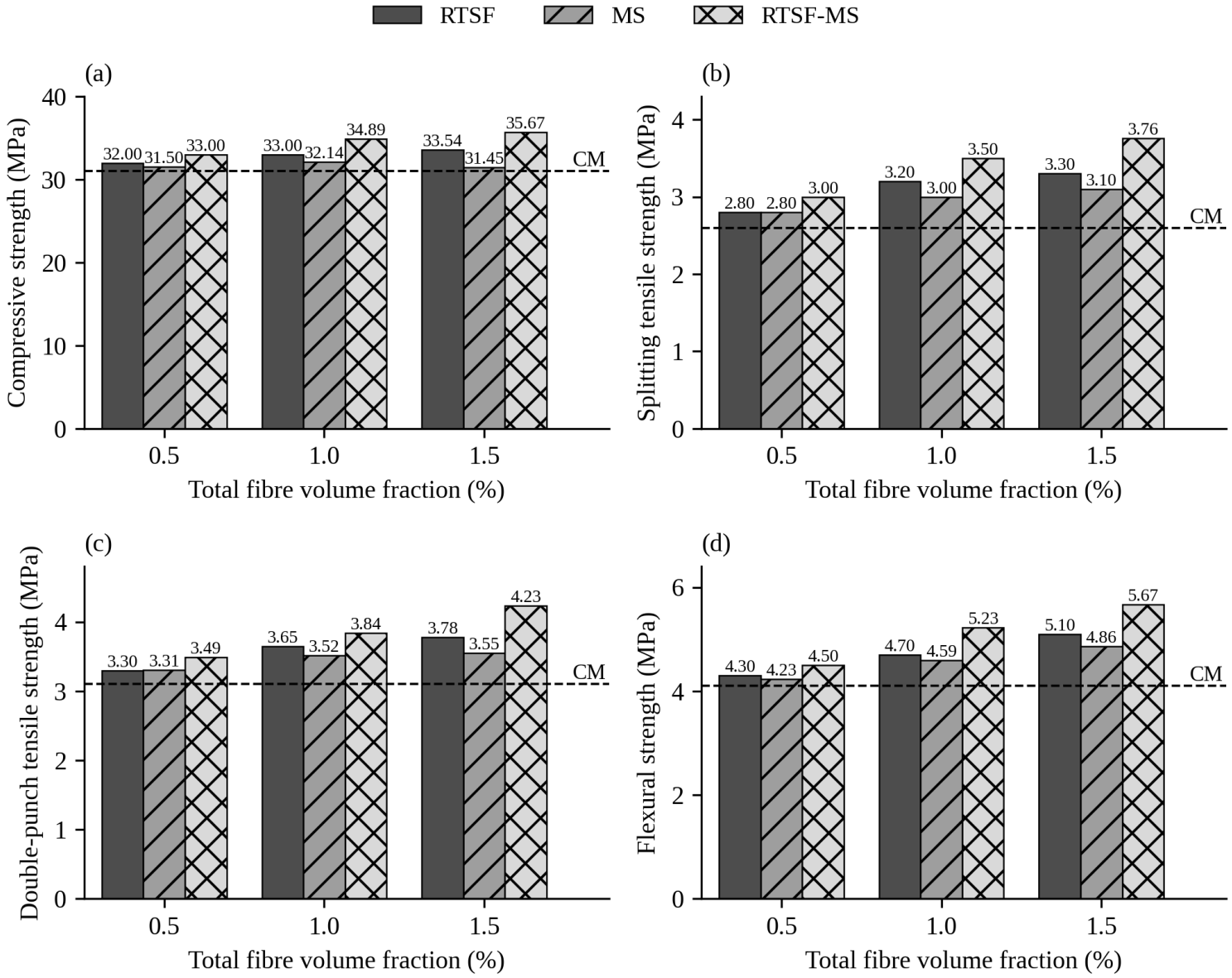


Figure 9. Mean 28-day strengths of the fibre-reinforced mixtures: (a) compressive; (b) splitting tensile; (c) double-punch tensile; (d) flexural. The dashed line marks the control mixture.

The small effect of fibres on compressive strength is consistent with the general view that fibres mainly act after cracking, by restraining the lateral expansion and crack growth that precede crushing, rather than by changing the strength of the matrix itself [3, 4]. The magnitude of the RTSF effect falls within the range reported for recycled and industrial steel fibres at similar contents [19, 59]. The MS series behaved differently. Its non-monotonic response, with a slight decline from 1.0 to 1.5%, resembles the trend reported by Ali et al. [19] for RTSF beyond an intermediate dosage, and may reflect less efficient compaction or local clustering of the curled shavings as their volume increases. Clustering was not examined in the fractured specimens, so this explanation is tentative. Because the MS changes are all within 3.7% of the control and no scatter data are available, they may not be distinguishable from normal batch variation.

The hybrid result is less easy to explain. The 1.5% hybrid exceeded both of its single-fibre counterparts (33.54 MPa for RTSF-1.5 and 31.45 MPa for MS-1.5) even though it had the lowest slump of all mixtures. Although the hybrid mixtures exhibited lower slump, their measured compressive strengths were higher than those of the corresponding single-fibre mixtures. This indicates that the lower slump did not coincide with a reduction in measured strength under the laboratory preparation conditions. However, because air content, void distribution and compaction efficiency were not measured directly, the adequacy of compaction cannot be established from compressive strength alone.

. A possible contribution is that the two fibre types, acting at different scales, provided more effective confinement of the microcracking that develops before peak load. This interpretation is consistent with the tensile results discussed below but cannot be confirmed from compressive tests alone, and the size of the increase warrants confirmation with replicate data.

3.3. Splitting tensile strength

Splitting tensile strength was the most sensitive property (Figure 10(b)). From 2.60 MPa for the control, it increased to 2.80, 3.20 and 3.30 MPa with RTSF (+7.7, +23.1 and +26.9%), to 2.80, 3.00 and 3.10 MPa with MS (+7.7, +15.4 and +19.2%) and to 3.00, 3.50 and 3.76 MPa with the hybrid (+15.4, +34.6 and +44.6%). The ratio of splitting to compressive strength rose accordingly, expressed as $f_{ct}/\sqrt{f_c}$, from 0.47 for the control to 0.57 for RTSF-1.5, 0.55 for MS-1.5 and 0.63 for the hybrid.

In the splitting test the specimen fails along the loaded diameter once the transverse tensile stress reaches the tensile capacity of the matrix. Fibres crossing that plane carry part of the stress as the first microcracks open and delay their coalescence into a through-crack, which

raises the peak load [4]. The higher mean splitting tensile strengths of the RTSF mixtures relative to the corresponding MS mixtures at 1.0 and 1.5% may be associated with differences in fibre geometry, length and orientation relative to the developing crack. However, fibre anchorage and pull-out behaviour were not measured directly, so this explanation remains tentative.

The shavings are shorter on average, and their ribbon cross-section and curled form mean that only part of each piece is aligned with the tensile stress. At 0.5% the two fibres gave the same result, suggesting that at low dosage the number of fibres crossing the failure plane, rather than their geometry, limited the response. The magnitude of the RTSF effect is lower than the 82% reported by Ali et al. [19] for twisted recycled fibres at 1.5% in a high-strength matrix, and similar to the increases reported by Şengül [18]. The MS results fall within the broad range reported by Małek et al. [27].

The hybrid gains were the largest measured in this study. At 1.0% the hybrid (0.5% RTSF + 0.5% MS) reached 3.50 MPa, higher than RTSF-1.5 (3.30 MPa), which contained 50% more fibre. This comparison is the clearest indication in the dataset that combining the two materials was more effective than increasing the dosage of either alone. A mechanism consistent with the hybrid concept is that the more numerous shavings restrain early microcracking while the longer tyre fibres bridge the localizing crack [31], but the present tests measured only peak load and cannot separate these stages.



Figure 10 Splitting tensile failure behaviour

3.4. Double-punch tensile strength

The double-punch strengths (Figure 6) followed the same ranking as the splitting results. From 3.10 MPa for the control they increased to 3.30, 3.65 and 3.78 MPa with RTSF (+6.5, +17.7 and +21.9%), to 3.31, 3.52 and 3.55 MPa with MS (+6.8, +13.5 and +14.5%) and to 3.49, 3.84 and 4.23 MPa with the hybrid (+12.6, +23.9 and +36.5%). The relative gains were somewhat smaller than in the splitting test for the single-fibre mixtures at 1.0 and 1.5%. The peak loads corresponding to these strengths, back-calculated from Eq. (4) with the specimen and punch dimensions, are listed in Table 7. They range from 132.2 kN for the control to 180.4 kN for RTSF-MS-1.5.

Table 7. Peak double-punch loads from the measured double-punch strengths with Eq. (4) (a = 19.05 mm, b = 76.2 mm, H = 152.4 mm).

Mix ID	f_{dp} (MPa)	Peak load P (kN)
CM	3.10	132.2
RTSF-0.5	3.30	140.7
RTSF-1.0	3.65	155.6
RTSF-1.5	3.78	161.2
MS-0.5	3.31	141.1
MS-1.0	3.52	150.1
MS-1.5	3.55	151.4
RTSF-MS-0.5	3.49	148.8
RTSF-MS-1.0	3.84	163.7
RTSF-MS-1.5	4.23	180.4

$P = f_{dp}\,\pi(1.2bH - a^2)$. Loads are derived from the reported strengths, not read from the test records.

The two tests load the specimen differently. In the splitting test, failure is forced along one predefined diametral plane. In the double-punch test, the conical wedges formed under the punches generate circumferential tension, and the specimen can fail along two or more radial planes whose orientation is not imposed [49]. Fibres are therefore engaged on several planes, and the test is less sensitive to the local fibre content at a single section. This may explain why the MS series, whose response flattened between 1.0 and 1.5%, showed the smallest increase in this test. The double-punch values were 10 to 19% higher than the corresponding splitting values for every mixture. The two results come from different stress states, specimen sizes (152.4 mm × 152.4 mm against 101.6 mm × 203.2 mm) and conversion formulas, and the double-punch expression is a limit-analysis approximation [51], so the ratio should not be interpreted as a difference in material behaviour. What matters for the present comparison is that the ranking of the mixtures is consistent between the two tests.

3.5. Flexural strength

Flexural strength increased with fibre content in all three series (Figure 9(d)). From 4.10 MPa for the control, it reached 4.30, 4.70 and 5.10 MPa with RTSF (+4.9, +14.6 and +24.4%), 4.23, 4.59 and 4.86 MPa with MS (+3.2, +12.0 and +18.5%) and 4.50, 5.23 and 5.67 MPa with the hybrid (+9.8, +27.6 and +38.3%). Unlike compressive and double-punch strength, flexural strength increased steadily with dosage for every fibre type, with no sign of levelling off within the investigated range.

Under four-point loading the whole middle third of the beam carries the maximum moment, so the critical crack initiates at the weakest section of that zone and the peak load is reached when it begins to propagate unstably. Fibres near the tension face resist the opening of this crack and redistribute stress to the uncracked section, which raises the modulus of rupture [3, 4]. Because the failure section is not fixed, the test is also sensitive to local variations in fibre content along the beam. In a 101.6 mm deep mould, the fibres close to the mould walls tend to align parallel to them [66]. For the 25 mm RTSF this wall effect favours orientation along the beam axis, which is the most effective direction for flexural reinforcement and may partly explain why RTSF gave larger gains than MS. The flexural gains are of the same order as those reported for RTSF by Centonze et al. [15] and Samarakoon et al. [59], and the MS gains fall within the range of Małek et al. [27] It should be emphasised that these results describe only the peak strength. The main advantage of steel fibres in flexure lies in the residual strength after cracking [15], which was not measured here.

The control modulus of rupture was $0.74\sqrt{f_c}$. This is above the $0.62\sqrt{f_c}$ commonly used in design, which is intended as a lower-bound estimate, and within the range usually measured for normal-strength concrete under third-point loading [1, 2].

3.6. Consistency among the tensile-related tests

Because each test engages the fibres in a different stress field, agreement among them provides a check on the reliability of the observed trends. The three tensile-related measures were strongly correlated (Figure 11). Flexural strength was related to splitting tensile strength by $f_r = 1.39f_{ct} + 0.41$ ($R^2 = 0.965$), and double-punch strength by $f_{dp} = 0.91f_{ct} + 0.74$ ($R^2 = 0.983$). The ratio f_r/f_{ct} varied only between 1.47 and 1.58 across all ten mixtures, indicating that the fibres raised all three measures in similar proportion. Compressive strength was also correlated with splitting strength ($R^2 = 0.87$), but the range of compressive values was much narrower.

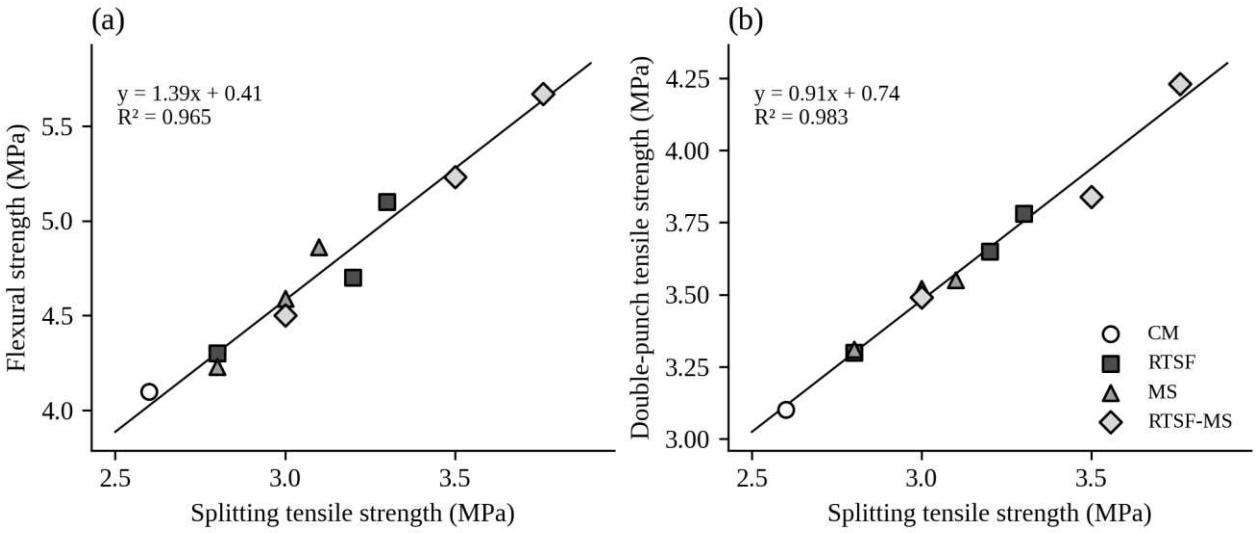


Figure 11. Relationship between splitting tensile strength and (a) flexural strength and (b) double-punch tensile strength for all ten mixtures.

The tests differed mainly in how the MS series behaved at the highest dosage. Its response flattened between 1.0 and 1.5% in compression and in the double-punch test, but continued to rise in splitting and flexure. Two factors may contribute. Flexural and splitting failures are controlled by a single dominant crack, whose resistance increases with the number of fibres crossing it, whereas compressive and double-punch failures involve distributed cracking over a larger volume, where clustering and local voids have more influence. These differences are small relative to the overall trends, and without an analysis of scatter it is not possible to say whether they are significant. Typical failure patterns are shown in Figure 10: the cylinders failed in compression with inclined cracking, the splitting specimens along a single diametral crack, the double-punch specimens along several radial cracks and the beams by a single flexural crack. Specimen-level observations of fibre pull-out or rupture were not recorded.

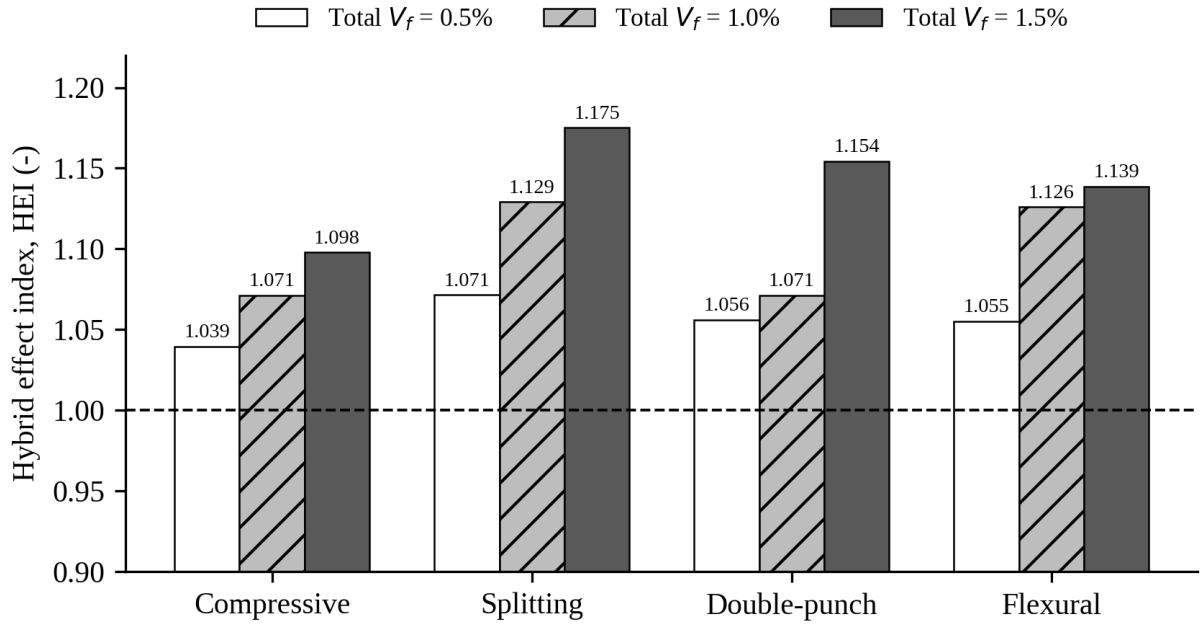
3.7. Behaviour of the hybrid system

The hybrid effect indices are listed in Table 8 and plotted in Figure 12. All twelve values are above 1.0, ranging from 1.039 (compression at 0.5%) to 1.175 (splitting at 1.5%), and in every property the index increased with total fibre content. In other words, each hybrid performed better than a proportional blend of its two components, and the margin widened as more fibre was added. The hybrids also exceeded the better of the two single-fibre mixtures in every case, which is a stricter criterion than the rule-of-mixtures comparison.

637 *Table 8. Hybrid effect index (HEI, Eq. (8)) for each property.*

Property	RTSF-MS-0.5	RTSF-MS-1.0	RTSF-MS-1.5
Compressive strength	1.039	1.071	1.098
Splitting tensile strength	1.071	1.129	1.175
Double-punch tensile strength	1.056	1.071	1.154
Flexural strength	1.055	1.126	1.139
Slump	0.959	0.898	0.859

638 HEI > 1 indicates that the hybrid exceeded the mean of the two single-fibre mixtures at the same total fibre volume fraction. For
639 slump, HEI < 1 indicates a larger loss of workability than the rule-of-mixtures expectation.
640



641
642 *Figure 12. Hybrid effect index (HEI, Eq. (8)) for each property and total fibre content. Values above 1.0*
643 *indicate that the hybrid exceeded the mean of its single-fibre counterparts.*

644 The questions posed in the introduction can now be answered for this matrix. Hybridisation
645 improved all three tensile-related properties, with HEI values of 1.06 to 1.18. It did not reduce
646 compressive strength; on the contrary, the hybrids gave the highest compressive values.
647 Flexural strength of the hybrids exceeded that of either single fibre at every dosage. The
648 workability penalty was also larger for the hybrids, since their slump was 4 to 14% below the
649 rule-of-mixtures expectation. The hybrid effect was therefore present in both the fresh and the
650 hardened state, beneficial in the latter and adverse in the former.

651 Whether this constitutes synergy in the sense used by Banthia and Gupta [32] depends on how
652 the evidence is weighed. The consistency of the result across four independent tests and three
653 dosages argues against chance. Against it, each value is the mean of three specimens from a
654 single batch, scatter was not analysed, and the mechanism was not observed. The most

655 defensible statement is that the data show a consistent positive hybrid effect at the level of
656 mean peak strength, which is compatible with complementary action of the two reinforcements
657 at different scales, and that its statistical significance remains to be established. The term
658 synergy is not used for this reason.

659 No formal optimization was carried out. Within the investigated range, RTSF-MS-1.5 was the
660 highest-performing mixture in every strength property but also had the lowest slump. RTSF-
661 MS-1.0 provides a useful alternative: with a total of 78.25 kg/m^3 of fibre, it matched or
662 exceeded RTSF-1.5 (117.15 kg/m^3) in all four strength measures (34.89 against 33.54 MPa in
663 compression, 3.50 against 3.30 MPa in splitting, 3.84 against 3.78 MPa in double-punch and
664 5.23 against 5.10 MPa in flexure) at practically the same slump (66 against 65 mm). Where the
665 design objective is tensile-related peak strength per unit of fibre, a moderate hybrid dosage
666 appears more efficient than a higher dosage of either material alone.

667 ***3.8. Carbon footprint***

668 The results of the CO_2 assessment are given in Table 9 and Figure 13. In scenario S1, cement
669 accounted for 340 of the 402.4 kg CO_2/m^3 of the control mixture (84.5%), followed by coarse
670 aggregate (47.6 kg, 11.8%), fine aggregate (8.5 kg, 2.1%) and superplasticizer (6.2 kg, 1.5%).
671 Because the cement content was constant and the fibres entered the system without burden,
672 fibre addition hardly changed the emissions per cubic meter. They fell by only 0.5% at 1.5%
673 fibre, from 402.4 to 400.5 kg CO_2/m^3, and only because a small amount of aggregate was
674 displaced. The result is the same for all three fibre types at equal dosage. On a volumetric basis,
675 therefore, reusing the waste steel did not reduce the footprint of the concrete; it simply did not
676 add to it.

677 *Table 9. Cradle-to-gate CO_2 emissions under scenario S1, carbon intensity, and emissions avoided*
678 *relative to an equal dosage of industrial steel fibres (scenario S2).*

Mix ID	S1 (kg CO_2/m^3)	S1/f_c	S1/f_r	Fibre mass (kg/m^3)	Avoided, scrap-EAF (kg CO_2/m^3)	Avoided, global avg. (kg CO_2/m^3)	Reduction vs industrial-fibre concrete (%)
CM	402.42	12.98	98.2	0.00	0.0	0.0	0
RTSF-0.5	401.77	12.56	93.4	39.05	26.9	75.0	6.3 to 15.7
RTSF-1.0	401.17	12.16	85.4	78.10	53.9	150.0	11.8 to 27.2
RTSF-1.5	400.53	11.94	78.5	117.15	80.8	224.9	16.8 to 36.0
MS-0.5	401.77	12.75	95.0	39.20	27.0	75.3	6.3 to 15.8
MS-1.0	401.17	12.48	87.4	78.40	54.1	150.5	11.9 to 27.3
MS-1.5	400.53	12.74	82.4	117.60	81.1	225.8	16.8 to 36.1
RTSF-MS-0.5	401.77	12.17	89.3	39.13	27.0	75.1	6.3 to 15.8
RTSF-MS-1.0	401.17	11.50	76.7	78.25	54.0	150.2	11.9 to 27.2

Mix ID	S1 (kg CO_2/m^3)	S1/f_c	S1/f_r	Fibre mass (kg/m^3)	Avoided, scrap-EAF (kg CO_2/m^3)	Avoided, global avg. (kg CO_2/m^3)	Reduction vs industrial-fibre concrete (%)
RTSF-MS-1.5	400.53	11.23	70.6	117.38	81.0	225.4	16.8 to 36.0

S1/f_c and S1/f_r in kg CO_2 m^{-3} MPa^{-1}. Avoided emissions = fibre mass × emission factor of industrial steel (Eq. (7)); the reduction is relative to the corresponding industrial-fibre concrete (E_{S2}). Transport is excluded in both scenarios.

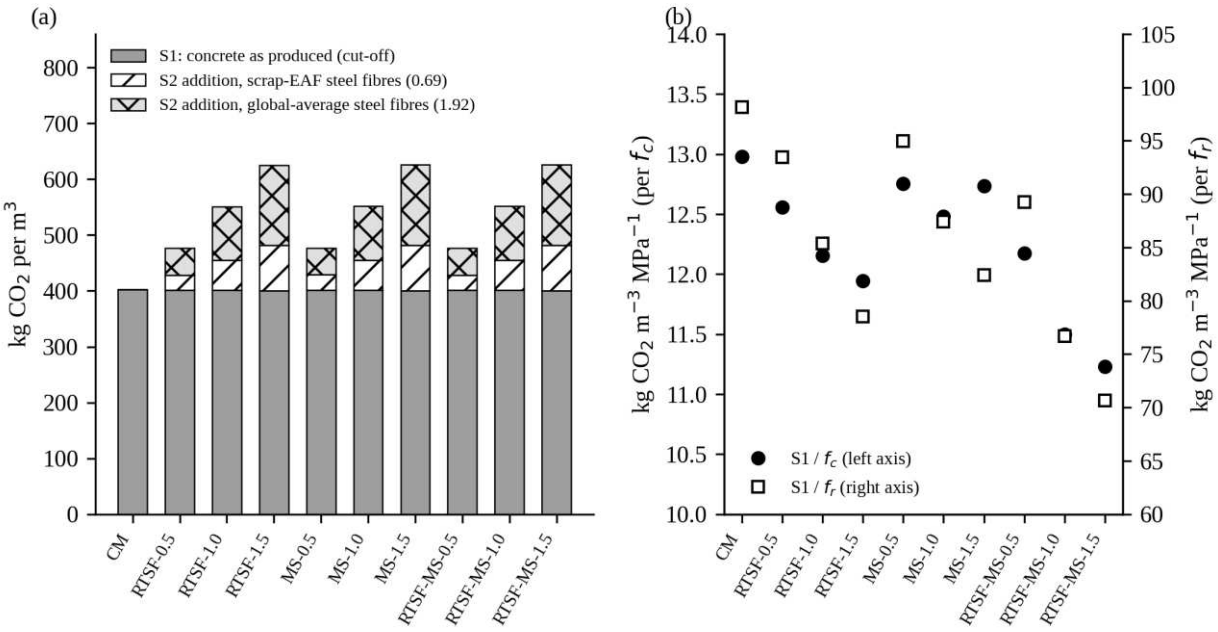


Figure 13. CO_2 assessment: (a) scenario S1 emissions per cubic metre, with the additional emissions that the same dosage of industrial steel fibres would cause (scenario S2) for the scrap-EAF and global-average steelmaking routes; (b) carbon intensity per unit compressive and flexural strength under S1.

The benefit becomes visible when emissions are related to performance. Since the strength gains came at no additional carbon cost, the S1 intensity per MPa of compressive strength fell from 12.98 kg CO_2 m^{-3} MPa^{-1} for the control to 11.94 for RTSF-1.5, 12.74 for MS-1.5 and 11.23 for RTSF-MS-1.5, a reduction of up to 13.5%. Per MPa of flexural strength the reduction was larger, reaching 28.0% for the 1.5% hybrid (from 98.2 to 70.6 kg CO_2 m^{-3} MPa^{-1}). These figures indicate a potential saving where a design is governed by flexural or tensile capacity and the higher strength allows a thinner section or a lower cement content, but such savings depend on the design case and were not demonstrated in this study.

Scenario S2 shows the magnitude of the benefit relative to the realistic alternative, a concrete reinforced with industrial steel fibres at the same dosage. Because S2 depends only on fibre mass, the result is practically identical for the three fibre types. At 0.5, 1.0 and 1.5% fibre, the waste fibres avoided about 27, 54 and 81 kg CO_2/m^3 if the industrial fibres were made from scrap-EAF steel, and about 75, 150 and 225 kg CO_2/m^3 if they were made from steel of average

global carbon intensity. Relative to the industrial-fibre concrete, these correspond to reductions of 6.3 to 16.8% and 15.7 to 36.1%, respectively. The upper end of this range is large because at 1.5% by volume the fibres weigh about 117 kg/m^3, and their emissions at the global-average intensity would amount to more than half of those of the cement.

Three qualifications apply to S2. First, the emission factors refer to crude steel and omit wire drawing and fibre forming, which makes the avoided emissions conservative. Second, the comparison is at equal dosage, not at equal performance; if industrial fibres achieved the same properties at a lower dosage, the avoided emissions would fall proportionally. Third, collection and transport of the waste fibres were not included in either scenario. Over regional distances these emissions are expected to be small compared with the totals in Table 9, and an equivalent transport burden would also apply to industrial fibres, but they should be included in a full assessment. Within these limits, the defensible conclusion is that the waste fibres offer their main environmental advantage by displacing industrial steel fibres, not by reducing the emissions of the concrete matrix itself.

4. Conclusions

Recycled tyre steel fibres, lathe metallic shavings and equal-volume hybrids of the two were compared at total fibre contents of 0.5, 1.0 and 1.5% by volume in a single normal-strength concrete. Within the limits of the programme, the following conclusions can be drawn.

(1) Slump decreased with total fibre content for all fibre types ($r = -0.94$), from 90 mm for the control to 65, 63 and 55 mm at 1.5% for RTSF, MS and the hybrid. At every dosage the hybrid gave the lowest slump, 4 to 14% below the mean of its single-fibre counterparts.

(2) Compressive strength was only modestly affected. It increased by up to 8.2% with RTSF, changed by no more than 3.7% with MS, with a slight decline from 1.0 to 1.5%, and increased by 6.5 to 15.1% with the hybrid.

(3) Splitting tensile strength was the most responsive property, increasing by up to 26.9% with RTSF, 19.2% with MS and 44.6% with the hybrid at 1.5%. RTSF were more effective than MS at 1.0 and 1.5%, whereas the two were equivalent at 0.5%.

(4) Double-punch tensile strength followed the same ranking, with increases of up to 21.9, 14.5 and 36.5% for RTSF, MS and the hybrid. Double-punch values were 10 to 19%

above splitting values for all mixtures, a difference attributed to test geometry and the conversion formula rather than to material behaviour.

(5) Flexural strength (modulus of rupture) increased steadily with dosage, by up to 24.4% with RTSF, 18.5% with MS and 38.3% with the hybrid.

(6) The three tensile-related measures were strongly correlated (R^2 = 0.965 for flexural and 0.983 for double-punch strength against splitting strength), so the observed trends were consistent across test configurations.

(7) All twelve hybrid effect indices exceeded 1.0 (1.04 to 1.18) and increased with dosage, and every hybrid outperformed both of its single-fibre counterparts. This consistent positive hybrid effect is compatible with complementary action of the two reinforcements, although its statistical significance could not be established.

(8) Within the investigated range, RTSF-MS-1.5 gave the highest strengths but the lowest slump. RTSF-MS-1.0 matched or exceeded RTSF-1.5 in all four strength measures with one third less fibre and similar slump.

(9) With the waste fibres treated as burden-free under a cut-off allocation, cradle-to-gate CO_2 emissions were essentially unchanged by fibre addition (402.4 to 400.5 kg CO_2/m^3), while the carbon intensity per MPa fell by up to 13.5% for compressive strength and 28.0% for flexural strength because of the strength gains. Compared with an equal dosage of industrial steel fibres, the waste fibres avoided about 27 to 226 kg CO_2/m^3, depending on dosage and on the steelmaking route assumed for the industrial fibres.

In practical terms, the results indicate that steel wastes from tyre recycling and machining can raise the tensile-related peak strengths of normal-strength concrete at dosages up to 1.5% by volume, and that combining them is more effective per unit of fibre than using either alone.

5. Limitations and future research

The conclusions are subject to several limitations that also define the most useful directions for further work.

Only peak strengths were measured. The principal function of steel fibres is to provide residual capacity after cracking, and load-deflection tests on notched or unnotched beams, for example according to ASTM C1609 or EN 14651, are needed before the materials can be assessed for structural use. The double-punch test with measurement of axial or circumferential

displacement, as in the Barcelona method, would also provide post-cracking information from cylinders.

Each property is reported as the mean of three specimens, and each mixture was produced in a single batch. Data from multiple batches and a statistical analysis of the scatter are required to test whether the hybrid effect and the small differences in compressive strength are significant.

The study used one concrete grade, one water-cement ratio and one curing age of 28 days. The influence of matrix strength, which strongly affects fibre efficiency, and of later ages remains to be examined.

The characterisation of the fibres was limited. The tensile strength of the shavings was taken from the specification of the parent steel, and their surface chemistry, residual oil content and the distribution of fibre dimensions were not measured, and the dispersion and orientation of fibres in the hardened concrete were not examined. Image analysis of sawn sections and microstructural examination of the fibre-matrix interface would help to confirm the mechanisms proposed here, particularly the entanglement of shavings with tyre fibres and the clustering of shavings at high dosage.

The carbon assessment was limited to the production of the constituents (module A1), used emission factors from different published sources and excluded fibre collection and transport. A full life cycle assessment with a consistent background database, regional data for cement production, and a functional unit tied to structural performance would give a more reliable comparison. Testing industrial steel fibres in the same matrix would also allow the substitution scenario to be evaluated at equal performance rather than equal dosage.

Finally, all tests were carried out on small laboratory specimens. Tests on structural elements, such as slabs on grade or beams with reduced conventional reinforcement, are needed to determine whether the material-level gains translate into useful structural performance.

Statements and Declarations

Consent

Ethics, Consent to Participate, and Consent to Publish declarations: Not applicable.

Data Availability

The datasets generated during and/or analysed during the current study are available from the corresponding author on reasonable request..

Competing Interests: The authors declare that they have no financial or non-financial competing interests that are directly or indirectly related to the work submitted for publication.

Funding: This research received no specific grant from any funding agency in the public, commercial, or not-for-profit sectors.

Author Contributions

Ahmad Subhan; Conceptualization, Methodology, Validation, Investigation, writing original draft, writing review and editing **Mirza Shariq**; Conceptualization, Methodology, Validation, Investigation, writing original draft, writing review and editing, visualization and supervision. **Naveed Ahmad:** Methodology, writing original draft and visualization. **Fatima Mehwish:** Conceptualization, Investigation, writing original draft and data curation.

Acknowledgments

The authors gratefully acknowledge the Department of Civil Engineering Structures, National University of Sciences and Technology (NUST), Islamabad, Pakistan, for providing structural testing facilities and BZU Multan, Pakistan, for providing access to the concrete laboratory facilities. The experimental support extended by both institutions was instrumental in the successful completion of this research.

Generative AI Use

Generative AI was used exclusively for language editing and sentence refinement. The authors take full responsibility for the accuracy, originality, and scientific content of the manuscript.

6. References

1. Scott, R., *Book review: Properties of Concrete, 5th edn*. 2013, Thomas Telford Ltd.
2. P Kumar Mehta, P.J., *Concrete microstructure, properties, and materials*. 2006: McGraw-hill.
3. 544, A.C., *Report on Fiber Reinforced Concrete*. 1996, American Concrete Institute: Farmington Hills, MI.
4. Bentur, A. and S. Mindess, *Fibre Reinforced Cementitious Composites.* Taylor & Francis/CRC Press, 1990.DOI: 10.1201/9781482267747.
5. Song, P. and S. Hwang, *Mechanical properties of high-strength steel fiber-reinforced concrete.* Construction and Building Materials, 2004. **18**(9): p. 669-673.
6. Yazıcı, Ş., G. İnan, and V. Tabak, *Effect of aspect ratio and volume fraction of steel fiber on the mechanical properties of SFRC.* Construction and Building Materials, 2007. **21**(6): p. 1250-1253.
7. Thomas, J. and A. Ramaswamy, *Mechanical properties of steel fiber-reinforced concrete.* Journal of materials in civil engineering, 2007. **19**(5): p. 385-392.
8. Environment, U., K.L. Scrivener, V.M. John, and E.M. Gartner, *Eco-efficient cements: Potential economically viable solutions for a low-CO2 cement-based materials industry.* Cement and concrete Research, 2018. **114**: p. 2-26.

9. Pilakoutas, K., K. Neocleous, and H. Tlemat. *Reuse of tyre steel fibres as concrete reinforcement*. in *Proceedings of the Institution of Civil Engineers-Engineering Sustainability*. 2004. Thomas Telford Ltd.
10. Neocleous, K., H. Tlemat, and K. Pilakoutas, *Design issues for concrete reinforced with steel fibers, including fibers recovered from used tires.* Journal of materials in civil engineering, 2006. **18**(5): p. 677-685.
11. Hu, H., et al., *Mechanical properties of SFRC using blended recycled tyre steel cords (RTSC) and recycled tyre steel fibres (RTSF).* Construction and Building Materials, 2018. **187**: p. 553-564.
12. Papakonstantinou, C.G. and M.J. Tobolski, *Use of waste tire steel beads in Portland cement concrete.* Cement and concrete research, 2006. **36**(9): p. 1686-1691.
13. Aiello, M.A., F. Leuzzi, G. Centonze, and A. Maffezzoli, *Use of steel fibres recovered from waste tyres as reinforcement in concrete: Pull-out behaviour, compressive and flexural strength.* Waste management, 2009. **29**(6): p. 1960-1970.
14. Tlemat, H., K. Pilakoutas, and K. Neocleous, *Stress-strain characteristic of SFRC using recycled fibres.* Materials and structures, 2006. **39**(3): p. 365-377.
15. Centonze, G., M. Leone, and M.A. Aiello, *Steel fibers from waste tires as reinforcement in concrete: A mechanical characterization.* Construction and Building Materials, 2012. **36**: p. 46-57.
16. Graeff, A.G., K. Pilakoutas, K. Neocleous, and M.V.N. Peres, *Fatigue resistance and cracking mechanism of concrete pavements reinforced with recycled steel fibres recovered from post-consumer tyres.* Engineering Structures, 2012. **45**: p. 385-395.
17. Leone, M., et al., *Fiber-reinforced concrete with low content of recycled steel fiber: Shear behaviour.* Construction and Building Materials, 2018. **161**: p. 141-155.
18. Sengul, O., *Mechanical behavior of concretes containing waste steel fibers recovered from scrap tires.* Construction and Building Materials, 2016. **122**: p. 649-658.
19. Ali, B., et al., *Effect of type and volume fraction of recycled-tire steel fiber on durability and mechanical properties of concrete.* European Journal of Environmental and Civil Engineering, 2023. **27**(5): p. 1919-1940.
20. Zhang, Y. and L. Gao, *Influence of tire-recycled steel fibers on strength and flexural behavior of reinforced concrete.* Advances in Materials Science and Engineering, 2020. **2020**(1): p. 6363105.
21. Liew, K. and A. Akbar, *The recent progress of recycled steel fiber reinforced concrete.* Construction and Building Materials, 2020. **232**: p. 117232.
22. Amjad, S., N. Ahmad, and H. Nawaz, *Combined Utilization of Crumb Rubber and Sulfuric Acid Treated Recycled Aggregate in Self-Compacting Concrete: Rheological, Mechanical, and Embodied Carbon Performance.* Frontiers in Engineering, Science & Management, 2026. **1**(1): p. 51-64.
23. Chantal, R., et al., *Environmental Assessment of Metal Chip Recycling – Quantification of Mechanical Processing's Global Warming Potential.* Procedia CIRP, 2024. **122**: p. 241-246.DOI: https://doi.org/10.1016/j.procir.2024.02.009.
24. Zainab, Z.I. and A.A.L.H. Enas, *Reuse of waste iron as a partial replacement of sand in concrete.* Waste Management, 2008. **28**(11): p. 2048-2053.DOI: https://doi.org/10.1016/j.wasman.2007.07.009.
25. Mohamed, A. and N. Jan, *Recycling of scale and steel chips waste as a partial replacement of sand in concrete.* Construction and Building Materials, 2012. **28**(1): p. 157-163.DOI: https://doi.org/10.1016/j.conbuildmat.2011.08.047.
26. Mohamed, A., *The implementation of scale and steel chips waste as a replacement for raw sand in concrete manufacturing.* Journal of Cleaner Production, 2016. **137**: p. 1038-1044.DOI: https://doi.org/10.1016/j.jclepro.2016.07.211.

27. Małek, M., et al., *Effect of metal lathe waste addition on the mechanical and thermal properties of concrete.* Materials, 2021. **14**(11): p. 2760.
28. Los Santos-Ortega, J., E. Fraile-García, J. Ferreiro-Cabello, and C. González-González, *Mechanical and environmental assessment of lathe waste as an addiction to concrete compared to the use of commercial fibres.* Materials, 2023. **16**(17): p. 5740.
29. Djebri, N., Z.E.A. Rahmouni, N.E. Djiab, and F. Haffaf. *The effect of the use of residues (metallic shavings) in the formulation of self-compacting concrete in fresh and hardened state*. in *Annales de Chimie. Science des Materiaux*. 2022. International Information and Engineering Technology Association (IIETA).
30. Aslan, Ç., Ö. Karagöz, H. Gökdemir, and A. Günaydın, *Effect of industrial waste metal chips on flexural behavior of reinforced concrete beams.* Revista de la construcción, 2023. **22**(2): p. 368-381.
31. Rossi, P., P. Acker, and Y. Malier, *Effect of steel fibres at two different stages: the material and the structure.* Materials and structures, 1987. **20**(6): p. 436-439.
32. Banthia, N. and R. Gupta, *Hybrid fiber reinforced concrete (HyFRC): fiber synergy in high strength matrices.* Materials and structures, 2004. **37**(10): p. 707-716.
33. Banthia, N. and M. Sappakittipakorn, *Toughness enhancement in steel fiber reinforced concrete through fiber hybridization.* Cement and concrete research, 2007. **37**(9): p. 1366-1372.
34. Yao, W., J. Li, and K. Wu, *Mechanical properties of hybrid fiber-reinforced concrete at low fiber volume fraction.* Cement and concrete research, 2003. **33**(1): p. 27-30.
35. Sivakumar, A. and M. Santhanam, *Mechanical properties of high strength concrete reinforced with metallic and non-metallic fibres.* Cement and Concrete Composites, 2007. **29**(8): p. 603-608.
36. Bjegovic, D., et al., *Positive interaction of industrial and recycled steel fibres in fibre reinforced concrete.* Journal of Civil Engineering and Management, 2013. **19**(sup1): p. S50-S60.
37. Martinelli, E., A. Caggiano, and H. Xargay, *An experimental study on the post-cracking behaviour of Hybrid Industrial/Recycled Steel Fibre-Reinforced Concrete.* Construction and Building Materials, 2015. **94**: p. 290-298.
38. Caggiano, A., et al., *On the mechanical response of hybrid fiber reinforced concrete with recycled and industrial steel fibers.* Construction and Building Materials, 2017. **147**: p. 286-295.
39. Zhong, H. and M. Zhang, *Experimental study on engineering properties of concrete reinforced with hybrid recycled tyre steel and polypropylene fibres.* Journal of Cleaner Production, 2020. **259**: p. 120914.
40. Molins, C., A. Aguado, and S. Saludes, *Double punch test to control the energy dissipation in tension of FRC (Barcelona test).* Materials and Structures, 2009. **42**(4): p. 415-425.
41. Authority, P.S.a.Q.C., *Specification for Ordinary Portland Cement (33, 43 and 53 Grades)*, in *PS 232:2008 (R)*. 2008, Pakistan Standards and Quality Control Authority: Islamabad, Pakistan.
42. International, A., *Standard Specification for Mixing Water Used in the Production of Hydraulic Cement Concrete*, in *ASTM C1602/C1602M*. 2022, ASTM International: West Conshohocken, PA.
43. International, A., *Standard Test Methods for Tension Testing of Metallic Materials*, in *ASTM E8/E8M*. 2024, ASTM International: West Conshohocken, PA.

44. International, A., *Standard Specification for Pipe, Steel, Black and Hot-Dipped, Zinc-Coated, Welded and Seamless*, in *ASTM A53/A53M*. 2022, ASTM International: West Conshohocken, PA.
45. Dixon, D.E., et al., *Standard practice for selecting proportions for normal heavyweight, and mass concrete (ACI 211.1-91) reapproved 1997.* Reported by ACI Committee, 1991. **211**: p. 1-38.
46. International, A., *Standard Test Method for Slump of Hydraulic-Cement Concrete*, in *ASTM C143/C143M*. 2020, ASTM International: West Conshohocken, PA.
47. International, A., *Standard Test Method for Compressive Strength of Cylindrical Concrete Specimens*, in *ASTM C39/C39M*. 2021, ASTM International: West Conshohocken, PA.
48. International, A., *Standard Test Method for Splitting Tensile Strength of Cylindrical Concrete Specimens*, in *ASTM C496/C496M*. 2017, ASTM International: West Conshohocken, PA.
49. Chen, W.-F. *Double punch test for tensile strength of concrete*. in *Journal Proceedings*. 1970.
50. de Normalización, A.E., *Hormigones con Fibras. Determinación de la Resistencia a Fisuración Tenacidad y Resistencia Residual a Tracción. Método Barcelona.* UNE, 2010. **83515**: p. 2010.
51. Chen, W.F. and R.L. Yuan, *Tensile strength of concrete: Double-punch test.* Journal of the Structural Division, 1980. **106**(8): p. 1673-1693.
52. Wei, X. and K.T. Chau, *Finite solid circular cylinders subjected to arbitrary surface load. Part II—Application to double-punch test.* International journal of solids and structures, 2000. **37**(40): p. 5733-5744.
53. Bortolotti, L., *Double-punch test for tensile and compressive strengths in concrete.* Materials Journal, 1988. **85**(1): p. 26-32.
54. International, A., *ASTM C78/C78M-22: Standard test method for flexural strength of concrete (using simple beam with third-point loading)*. 2022, ASTM International West Conshohocken, PA.
55. Standardization, I.O.f., *Environmental management Life cycle assessment Principles and framework*, in *ISO 14040:2006*. 2006, International Organization for Standardization: Geneva, Switzerland.
56. Standardization, I.O.f., *Environmental management — Life cycle assessment — Requirements and guidelines*, in *ISO 14044:2006*. 2006, International Organization for Standardization: Geneva, Switzerland.
57. Standardization, E.C.f., *Sustainability of construction works, Environmental product declarations, Core rules for the product category of construction products*, in *EN 15804:2012+A2:2019*. 2019, European Committee for Standardization: Brussels, Belgium.
58. Association, W.S., *Sustainability Indicators 2025 Report*, in *Sustainability Indicators 2025 Report*, W.S. Association, Editor. 2025: Brussels, Belgium.
59. Samarakoon, S.S.M., P. Ruben, J.W. Pedersen, and L. Evangelista, *Mechanical performance of concrete made of steel fibers from tire waste.* Case Studies in Construction Materials, 2019. **11**: p. e00259.
60. Wu, L., et al., *Influence of recycled tire steel fibers on the mechanical properties and carbon emissions of high-performance cement-based materials.* Materials, 2025. **18**(13): p. 3008.
61. Flower, D.J. and J.G. Sanjayan, *Green house gas emissions due to concrete manufacture.* The international Journal of life cycle assessment, 2007. **12**(5): p. 282-288.

62. Damineli, B.L., F.M. Kemeid, P.S. Aguiar, and V.M. John, *Measuring the eco-efficiency of cement use.* Cement and Concrete Composites, 2010. **32**(8): p. 555-562.
63. Association, W.S., *Sustainability Indicators 2025 Report*. 2025, World Steel Association: Brussels, Belgium.
64. Martinie, L., P. Rossi, and N. Roussel, *Rheology of fiber reinforced cementitious materials: classification and prediction.* Cement and concrete research, 2010. **40**(2): p. 226-234.
65. Ferrara, L., Y.-D. Park, and S.P. Shah, *A method for mix-design of fiber-reinforced self-compacting concrete.* Cement and concrete research, 2007. **37**(6): p. 957-971.
66. Soroushian, P. and C.-D. Lee, *Distribution and orientation of fibers in steel fiber reinforced concrete.* Materials journal, 1990. **87**(5): p. 433-439.